frontiers | Frontiers in Veterinary Science

TYPE Original Research
PUBLISHED 08 August 2023
DOI 10.3389/fvets.2023.1142305

OPEN ACCESS

EDITED BY
Marianna Santonastaso,
Università degli Studi della Campania Luigi Vanvitelli, Italy

REVIEWED BY
Anna Zielak-Steciwko,
Wroclaw University of Environmental and Life Sciences, Poland
Aziza Abdel-Salam El-Nekeety,
National Research Centre, Egypt
Francesca Marcon,
National Institute of Health (ISS), Italy

*CORRESPONDENCE
Ibrahim F. Rehan
✉ ibrahim.rehan@vet.menofia.edu.eg
František Zigo
✉ frantisek.zigo@uvlf.sk

RECEIVED 11 January 2023
ACCEPTED 13 July 2023
PUBLISHED 08 August 2023

CITATION
Kamal Z, Said AH, Ebnalwaled AA, Rehan IF, Zigo F, Farkašová Z and Allam M (2023) Genetic effects of chemically and biosynthesized titanium dioxide nanoparticles *in vitro* and *in vivo* of female rats and their fetuses. *Front. Vet. Sci.* 10:1142305. doi: 10.3389/fvets.2023.1142305

Genetic effects of chemically and biosynthesized titanium dioxide nanoparticles *in vitro* and *in vivo* of female rats and their fetuses

Zeinab Kamal[1], Alaa H. Said[2], A. A. Ebnalwaled[2], Ibrahim F. Rehan[3,4]*, František Zigo[5]*, Zuzana Farkašová[5] and Mohammad Allam[6]

[1]Department of Zoology, Faculty of Science, South Valley University, Qena, Egypt, [2]Electronic and Nano Devises Lab, Faculty of Science, South Valley University, Qena, Egypt, [3]Department of Husbandry and Development of Animal Wealth, Faculty of Veterinary Medicine, Menoufia University, Shebin Alkom, Egypt, [4]Department of Pathobiochemistry, Faculty of Pharmacy, Meijo University, Nagoya, Aichi, Japan, [5]Department of Nutrition and Animal Husbandry, University of Veterinary Medicine and Pharmacy in Košice, Košice, Slovakia, [6]Department of Zoology, Faculty of Science, Luxor University, Luxor, Egypt

With the increase in nanoparticles (NPs) products on the market, the possibility of animal and human exposure to these materials will increase. The smaller size of NPs facilitates their entrance through placental barriers and allows them to accumulate in embryonic tissue, where they can then be a source of different developmental malformations. Several toxicity studies with chemically synthesized titanium dioxide NPs ($CTiO_2$ NPs) have been recently carried out; although there is insufficient data on exposure to biosynthesized titanium dioxide NPs ($BTiO_2$ NPs) during pregnancy, the study aimed to evaluate the ability of an eco-friendly biosynthesis technique using garlic extract against maternal and fetal genotoxicities, which could result from repeated exposure to TiO_2 NPs during gestation days (GD) 6–19. A total of fifty pregnant rats were divided into five groups (n = 10) and gavaged $CTiO_2$ NPs and $BTiO_2$ NPs at 100 and 300 mg/kg/day concentrations. Pregnant rats on GD 20 were anesthetized, uterine horns were removed, and then embryotoxicity was performed. The kidneys of the mothers and fetuses in each group were collected and then maintained in a frozen condition. Our results showed that garlic extract can be used as a reducing agent for the formation of TiO_2 NPs. Moreover, $BTiO_2$ NPs showed less toxic potential than $CTiO_2$ NPs in $HepG_2$ cells. Both chemically and biosynthesized TiO_2 NP-induced genetic variation in the *16S rRNA* sequences of mother groups compared to the control group. In conclusion, the genetic effects of the *16S rRNA* sequence induced by chemically synthesized TiO_2 NPs were greater than those of biosynthesized TiO_2 NPs. However, there were no differences between the control group and the embryo-treated groups with chemically and biologically synthesized TiO_2 NPs.

KEYWORDS

***16S rRNA*, titanium dioxide, developmental toxicity, biosynthesized, particle characterization**

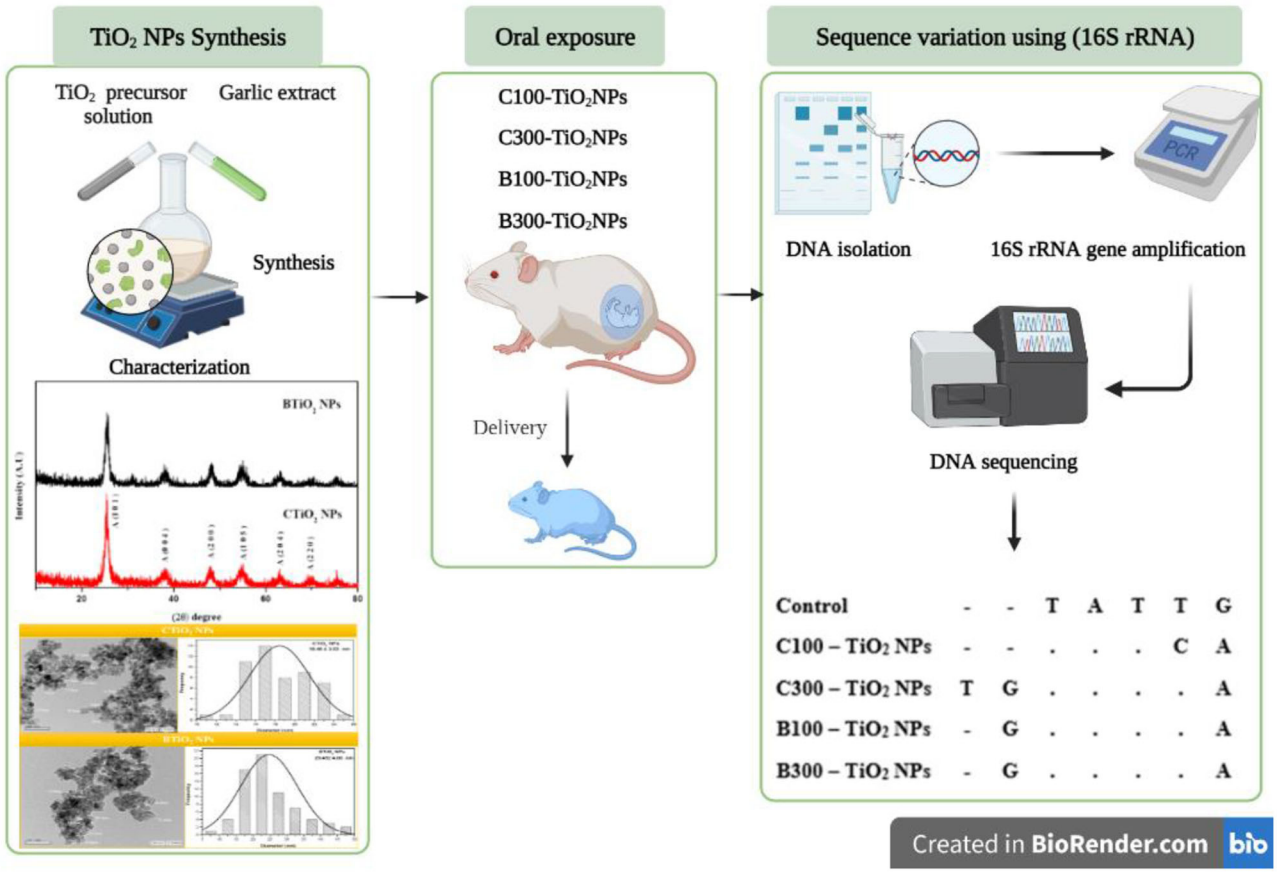

GRAPHICAL ABSTRACT
Schematic carton of the study showed the experimental strategy. It was designed by BioRender.com.

Introduction

In the coming decades, industrial production is expected to change as a result of the rapidly expanding field of nanotechnology. The high surface area and smaller particle size of NPs, along with their flexible design, functionalization, biocompatibility, and bioactivity, played a key role in tuning NPs in many applications. The major application is breaking the barriers among fundamental fields such as biology, chemistry, and physics. The application field is also expanding, including medical products, imaging techniques, sporting equipment, food production and agriculture, cosmetics, clothing cleaning products, personal care items, and toys for kids (1, 2). However, most nanomaterials have been introduced into the market based on claimed advantages, and the ecotoxicological potential of nanomaterial products is unclear to the scientific community (2, 3). The nanomaterials' physicochemical properties are due to their chemical nature, small size, surface composition, and aggregation (4).

For NP synthesis, there are two main approaches: the top-down method and the bottom-up method (5). The top-down approach starts with size reduction from the bulk material to the nanosized with physical methods such as ball milling and laser ablation (6), while the bottom-up approach needs a reducing agent to decrease the size of the particle. Chemical (for example, sodium hydroxide and potassium hydroxide) and biological [biomolecules from bacteria (6), fungi (7), yeast (8), virus (9), and plant extracts (10)] reducing agents can work perfectly for controlling the size of metals and metal oxides. Biomolecules are preferred due to their safety and biocompatibility with DNA, proteins, enzymes, polyphenols, flavonoids, and sugars (11). The simplest and quickest way to create NPs, which are based on the proteins and carbohydrates in biomolecules and act as a reducing agent to encourage the synthesis of metallic nanoparticles, is through plant extracts (12). Biomolecules have many chemically active groups such as hydroxyl, amine, and thiol groups (13). These groups will interact with metal ions in the solution via electron transfer, leading to oxidization from a positive oxidization state to a zero oxidization state, which guides the nucleation process.

Abbreviations: NPs, Nanoparticles; ROS, Reactive Oxygen Species; TTIP, Titanium isopropoxide; $BTiO_2$ NPs, Biosynthesized titanium dioxide NPs; $CTiO_2$ NPs, Chemically synthesized titanium dioxide NPs; GD, Gestation day; $HepG_2$ cells, Liver hepatocellular cells; DMSO, Dimethylsulfoxide; XRD, X-ray diffraction; FWHM, Full width at half maximum; HRTEM, High-resolution transmission electron microscope; FTIR, Fourier transformation infrared; DMEM, Dulbecco's Modified Eagle's Medium; MTT, 3-[4,5-dimethylthiazol-2-yl]-2,5-diphenyltetrazolium; Large subunit ribosomal RNA, *16S rRNA* gene.

Comparing biosynthesized NPs with those made using chemical methods, the biocompatibility of these NPs allows for a wide range of biomedical applications (14).

Exposure to TiO_2 NPs may change the cell membrane due to oxidative stress or even *via* Van der Waal forces with the cell wall, leading to defragmentation of the cell membrane and molecular structure, which induces genetic variation (15, 16). The generated reactive oxygen species (ROS) also oxidize DNA, resulting in mutations in DNA (15, 17). In addition, reactive oxygen species may promote inflammation, and oxidative stress and inflammation result in cell apoptosis (16, 18).

Recently, several toxicity studies with chemically synthesized titanium dioxide nanoparticles ($CTiO_2$ NPs) have been performed. Organs such as the kidney, liver, and spleen can suffer damage due to exposure to TiO_2 NPs (19–21), such as inflammation of renal tissue due to ROS. In addition, TiO_2 NPs accumulate in the kidney tissues and cause changes in embryogenesis during the first trimester of pregnancy (22, 23). In addition, oxidative stress significantly increases with increasing TiO_2 NP concentrations (24).

A repeated oral administration of $CTiO_2$ NPs in other experimental animals showed disturbances in metabolism (25). The results of the studies performed on rats as animal models revealed that after absorption of $CTiO_2$ NPs can enter the systemic circulation and cause organ injuries and inflammation (26).

Several *in vivo* and *in vitro* studies were carried out to assess the toxicity of green TiO_2 NPs. The reported toxicological data proposed that green TiO_2 promotes a higher safety profile with improved anticancer, antibacterial, and antiviral activities compared with chemically synthesized TiO_2 NPs (27). However, there are limited toxicological data on exposure to biosynthesized TiO_2 NPs from garlic extract ($BTiO_2$ NPs) during pregnancy. This study is based on the new method of biosynthesis of TiO_2 NPs by using garlic extract as a reducing agent, performing *in vivo* investigations on pregnant rats and their fetuses, and comparing the toxicity of $BTiO_2$ NP synthesis with that of $CTiO_2$ NP synthesis in both *in vivo* and *in vitro*.

Materials and methods

Chemicals and reagents

The following chemicals and reagents were used without any purification: titanium isopropoxide (TTIP), Dulbecco's modified Eagle's medium (DMEM), and penicillin–streptomycin (P/S) were purchased from Sigma–Aldrich Co., USA. Fetal bovine serum (FBS) was purchased from Biochrom, and 0.05% Trypsin-EDTA was purchased from HiMedia, India. Phosphate-buffered saline (PBS) was purchased from Serox, Germany, and 3-(4,5-dimethylthiazol-2-yl)-2, 5-diphenyltetrazolium and DMSO were purchased from Lobalohemia, India. Qiagen DNA mini kit and 100 bp DNA Ladder were purchased from GeneDireX (Germany). Liver hepatocellular cells ($HepG_2$ cell lines) were purchased from VACSERA, Giza, Egypt.

Synthesis of chemical TiO_2 NPs ($CTiO_2$ NPs)

TiO_2 NPs were created chemically using the coprecipitation method (28). In brief, 5 ml of titanium isopropoxide (TTIP) in 15 ml of propanol was used as a precursor solution, while the solvent solution was a 50/1 (V/V) mixture of distilled water and propanol. The precursor solution was added dropwise to the solvent solution after it had been heated to 70–90°C under continuous stirring for 2 h. As soon as the TiO_2 precursor was reduced to form TiO_2 NPs, a white precipitate started to form. The precipitate was centrifuged and allowed to cool at room temperature for the entire next day. The final precipitate was, then, dried at 100°C for 12 h and calcined at 400°C for 3 h after being washed three times with distilled water and once with ethanol.

Biosynthesis of TiO_2 NPs using garlic extract ($BTiO_2$ NPs)

Garlic (*Allium sativum*) water extract was used as a reducing agent for the biosynthesis of TiO_2 NPs. Approximately 20 g of washed and dried garlic in 150 ml of distilled water were boiled for 1 h to prepare the solvent solution. The precursor solution was prepared by adding 10 ml of TTIP to 150 ml of distilled water and vigorously stirring. Dropwise addition of a solvent solution (60 ml) of fresh garlic plant extract was made, while the precursor solution was continuously stirred for 2 h. The color of the solution changed from white to dark yellow, indicating that TTIP was reduced and $BTiO_2$ NPs were created. The formed precipitate was centrifuged and collected after being allowed to cool at room temperature for the entire night. The final precipitate was, then, dried at 100°C for 12 h and calcined at 400°C for 3 h after being washed three times with distilled water and once with ethanol.

TiO_2 NP characterizations

The produced TiO_2 NPs were categorized by X-ray diffraction (XRD) using X' Pert PRO-PAN, Malvern Panalytical, UK, diffractometer with cooper radiation (wavelength 1.54056 Å) at 40 kV and 30mA, high-resolution transmission electron microscopy (HETM) (JEOL, JEM 2100, Japan), Raman spectrometer (Horiba Jobin Yvon HR 800UV, Japan), and FTIR spectrophotometer (Model 6100, Jasco-Japan), with a resolution of 4.00 $cm^{-1}$and covers the wave number range of 4000–400 cm^{-1} was used to determine the functional groups in the prepared samples. The optical absorption spectra of the prepared samples were evaluated with a UV–visible spectrophotometer (SPECORD 200 PLUS, Analytik Jena, Germany).

Cell viability

Liver hepatocellular cells ($HepG_2$ cell lines) were obtained from Vacsera (Giza, Egypt). Cells were cultured in Dulbecco's modified Eagle's medium (DMEM, Sigma–Aldrich, #D5796), supplemented with 10% heat-inactivated fetal bovine serum (FBS, Biochrom,

#S0615) and 1% penicillin–streptomycin (P/S, Sigma–Aldrich, #P4333). Cells were grown in 75 cm^2 flasks (VACSERA Center, Cairo) and sub-cultured at approximately 80% confluency.

MTT assay was used to assess the mitochondrial function by reducing the tetrazolium dye MTT 3-(4, 5-dimethylthiazol-2-yl)-2, 5-diphenyltetrazolium to the insoluble magenta formazan where a yellow tetrazolium is reduced to purple formazan in living cells (29). $HepG_2$ cells were seeded in 96-well culture plates with a total density of 1×10^4 cells per well and incubated at 37°C and 5% CO_2. After 24 h of incubation, the culture medium was removed, and cells were rinsed with 100 µl PBS. Afterward, cells were exposed to both samples of TiO_2 NPs with different concentrations (0, 0.5, 1, 2, 4, and 8 mM) and then incubated at 37°C and 5% CO_2. After 24 h, cells were rinsed with PBS, and 80 µl of media without serum and 20 µl of MTT solution were added to each well and then incubated at 37°C for 3 h. Finally, the MTT solution was removed, then 100 µl of MTT solvent (DMSO) was added to each well, and the plates were warped in foil and shaken on an orbital shaker for 15 min. The absorbance at OD = 590 nm was recorded for each well with a Tecan infinite F50 absorbance microplate reader, and the cell viability was calculated using the following equation (29).

$$\text{Cell viability\%} = \frac{\text{Absorbance}_{\text{control}} - \text{Absorbance}_{\text{sample}}}{\text{Absorbance}_{\text{control}}}$$

Animal experiment

In total, 20–30-week-old healthy female Albino Sprague–Dawley rats, weighing 180–220 g, were obtained from the animal house of the National Research Center Institute (Cairo, Egypt). The rats were housed in cages made of plastic, using a bedding material made of a wooden dust-free litter, and permitted a 2-week period of acclimation before the beginning of the study under hygienic measures and standard conditions (25 ± 2○C room temperature, 50% ± 15% relative humidity, and light–dark cycle of 12 h). All rats were given a commercial pellet diet and water *ad libitum*.

Experimental design and treatment

The study aimed to assess the ameliorator abilities of an eco-friendly biosynthesizing method using garlic (*Allium sativum*) extract as a reducing agent against maternal and fetal genotoxicities that could develop from repeated oral administration of TiO_2 NPs in pregnant mothers between gestation days 6 and 19. In total, 50 adult female rats were selected for this study and mated at night using healthy males in a ratio of 1:3. The day that sperm was observed in the vaginal smear, the next morning was regarded as GD1. After pregnancy detection, pregnant females were weighed and assigned into five equal groups, each of which comprises 10 pregnant mothers, as follows:

Group 1: control group, administrated distilled water by gavage (1 ml/day).

Group 2 and *Group 3*: $CTiO_2$ NP-treated groups received 100 and 300 mg/kg body weight (bw)/day, (30, 31) respectively.

Group 4 and *Group 5*: $BTiO_2$ NP-treated groups received 100 and 300 mg/kg bw/day, respectively. These concentrations of TiO_2 NPs of 100 and 300 mg/kg bw were chosen according to the World Health Organization (WHO) in 1969 (32), which reported that the LD_{50} of TiO_2 for rats is greater than 12,000 mg/kg bw. Pregnant mothers were exposed to 100 mg/kg bw $CTiO_2$ NPs or $BTiO_2$ NPs, which is equal to approximately 6–7 g of TiO_2 NPs per 60–70 kg bw for humans (33).

TiO_2 NPs were suspended in distilled water. Throughout the dosing process, the dosage was continuously shaken to produce a homogenized suspension, and throughout the dosing procedure, the dosage was continuously stirred with a magnetic stirrer. All treatments were obtained by oral gavage and were freshly prepared. The pregnant rats' treatment starts from GD 6 to GD 19 (31). The schematic diagram of the study showed the experimental strategy (see Graphical abstract).

At the end of the experimental period on GD 20, all dams were euthanized by ether, and cesarean sections were performed. The uterine horns were removed, and then, the embryotoxicity was performed. The kidneys of mothers and fetuses in each group were collected and then maintained in a frozen condition.

DNA extraction, PCR amplification, and sequencing

Qiagen DNA mini kit was used to extract the genomic DNA from the kidneys of mothers and fetuses in each group by following the manufacturer's guidelines. The quality of DNA was examined by agarose gel electrophoresis with a 100bp DNA Ladder under UV light. The previous report stated that primers were used for *16S rRNA* amplification (34). The polymerase chain reaction was executed in a final reaction volume of 40 µl, adding 20 µl of 2X Master Mix, 1 µl of each forward and reverse primer, 17 µl of nuclease-free water, and 1 µl genomic DNA. The PCR conditions were as follows: denaturing at 95°C for 4 min, then 35 cycles of denaturing at 94°C for 60 s, annealing at 48°C for 60 s, extension at 72°C for 60 s, and finishing with an extension at 72°C for 7 min. Amplification was confirmed by means of agarose gel electrophoresis at 1.5% containing ethidium bromide. The DNA sequencing was executed by Macrogen (South Korea). Sequence alignment was implemented using Clustal W (35).

Biopsy of fetal kidney

Fetal kidney biopsies from all embryos were extracted and thoroughly dipped in formalin solution to be fixative, followed by serial dehydration in ethanol, and embedding in paraffin wax. Kidney sections of approximately 5 microns were stained with hematoxylin and eosin (H&E) for histological findings (36).

Results

X-ray diffraction

The biosynthesis of NPs is an emerging technique that produces NPs with unique properties. Green nanotechnology was applied to the synthesis of TiO_2 NPs, and the formed NPs were characterized

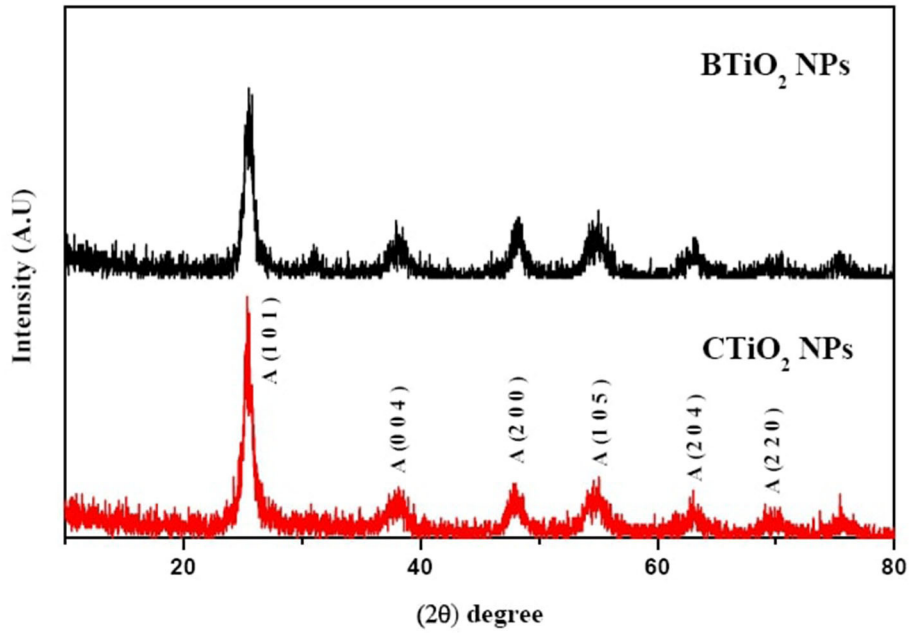

FIGURE 1
XRD patterns of $CTiO_2$ and $BTiO_2$ NPs.

by several techniques. Structural analysis using XRD, HRTEM, and Raman spectroscopy revealed anatase phase formation, which indicates the complete reduction of titanium isopropoxide using garlic extract. No additional peaks for impurities, such as NaCl and Na_2TiO_3, were observed, indicating the high purity of the prepared samples. The X-ray diffraction (XRD) pattern of TiO_2 NPs (see Figure 1) revealed the phase and structural purity of TiO_2 NPs. All the recorded peaks belong to the anatase phase TiO_2 NPs, which support the reported card (JCPDS No. 21-1272). Although the diffraction peak of brookite B (*121*) was found in $CTiO_2$ NPs, it disappeared in $BTiO_2$ NPs (37).

Debye–Scherer's equation was used for the calculation of the average crystal size of TiO_2 NPs (38).

$$d = \frac{0.89\lambda}{FWHM\ Cos\theta}$$

where d is the average crystal size of TiO_2 NPs, λ is the wavelength of X-rays, 0.89 is a constant, θ is the diffraction angle, and FWHM is the full width at half maximum of XRD peaks recorded at diffraction angle 2θ. The calculated average crystalline size of $CTiO_2$ NPs was 48.11 nm, while it was increased to 53.31 nm for $BTiO_2$ NPs.

UV–visible spectroscopy

Both $CTiO_2$ and $BTiO_2$ samples have absorption spectra in the region below 400 nm. The spectral image displays the absorption peaks of TiO_2 NPs at wavelengths of 261.87 and 314 nm for $CTiO_2$ and $BTiO_2$ NPs, respectively (see Figure 2).

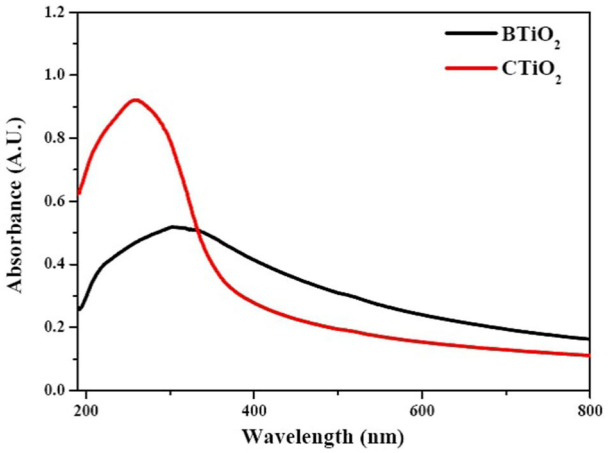

FIGURE 2
UV spectra of $BTiO_2$ and $CTiO_2$ NPs.

The optical band gap Eg of TiO_2 NPs was calculated by Tauc's equation (39) as follows:

$$\propto (h\nu) = A\left(h\nu - E_g\right)^{\frac{m}{2}}$$

where ∝ is the absorption coefficient of TiO_2 NPs, the energy of incident light of wavelength λ was $h\nu = hc/\lambda$, (A) was constant, and (m) depends on the nature of the transition.

The direct band gaps of $CTiO_2$ and $BTiO_2$ NPs were 3.544ev and 2.660ev, respectively (see Figure 3).

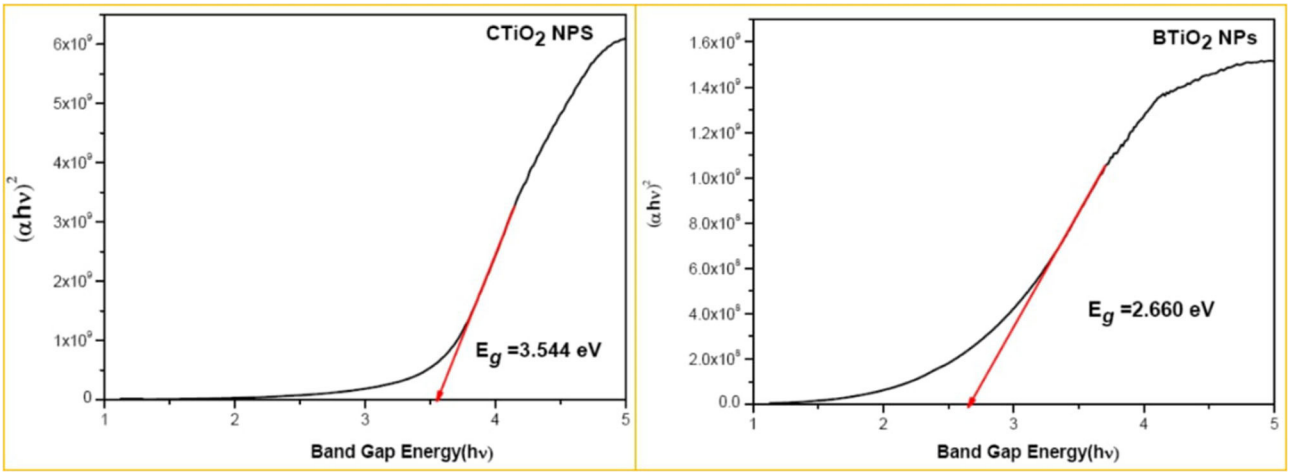

FIGURE 3
Optical band gap of $CTiO_2$ and $BTiO_2$ NPs.

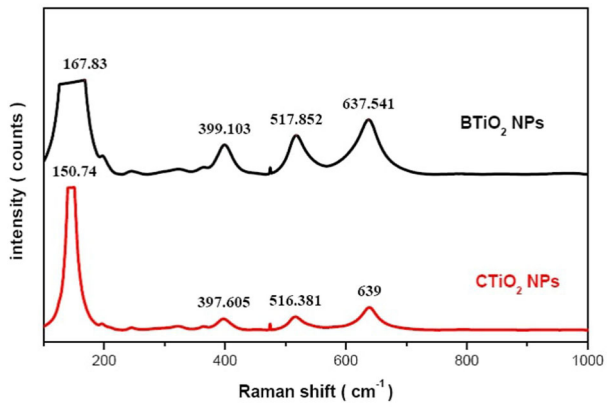

FIGURE 4
Raman spectra of $CTiO_2$ and $BTiO_2$ NPs.

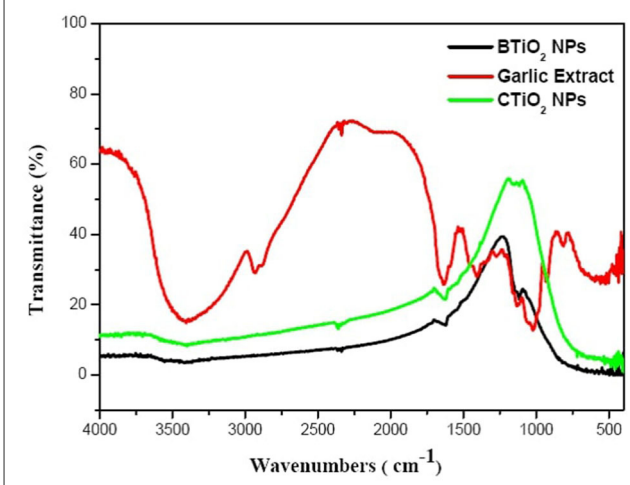

FIGURE 5
FTIR spectra of garlic extract and $BTiO_2$ and $CTiO_2$ NPs.

Raman spectra analysis of tio$_2$ NPs

The structural characterization of chemically and biosynthesized TiO_2 NPs with garlic extract by Raman spectroscopy is presented in Figure 3. The six active modes that belong to the anatase phase of TiO_2 were found in the two samples, which confirm the XRD result of the formation of anatase TiO_2 NPs. The low frequency O-Ti-O bending oscillation was observed for all samples as $E_{g(1)}$, $E_{g(2)}$, and B_{1g} modes (40). All sample frequency positions are higher than the reported values for bulk TiO_2 (143, 197, and 399 cm^{-1}, respectively). Moreover, higher frequency Ti-O strain oscillation was observed for all samples in $E_{g(3)}$ and A_{1g} modes. The frequency position of $E_{g(3)}$ has a lower frequency position than that of the bulk TiO_2 (639 cm^{-1}), while the frequency position of A_{1g} has a higher frequency position than that of the bulk TiO_2 (514 cm^{-1}). This result is attributed to a reduction in the crystal size of TiO_2 NPs that are produced chemically and biologically (41).

Fourier-transform infrared spectra

FTIR spectrum for $CTiO_2$ NPs is presented in Figure 4. The broad band at 3426.2 cm^{-1} is assigned to the vibration of the hydroxyl group (42). The vibration band at 1151cm^{-1} is due to Ti-O-Ti vibrations. The band at 1628 cm^{-1} is described as the bending vibration of adsorbed water and Ti-OH (43). A band at 1376 cm^{-1} is attributed to the asymmetrical C–H vibrations (43, 44). The band at 457.6 cm^{-1} corresponds to the Ti–O –Ti. Vibrational bands appearing around 723 cm^{-1} correspond to TiO_2 modes in the anatase phase (45–47).

FTIR spectrum of garlic extract was studied to identify the presence of garlic function groups. The band at 3415.5cm^{-1} describes the vibration of the hydroxyl group (O-H) and the presence of carbohydrates and amino acids. The bands at 2932 cm^{-1} and 2890.2 cm^{-1} represent the C-H stretching for lipids

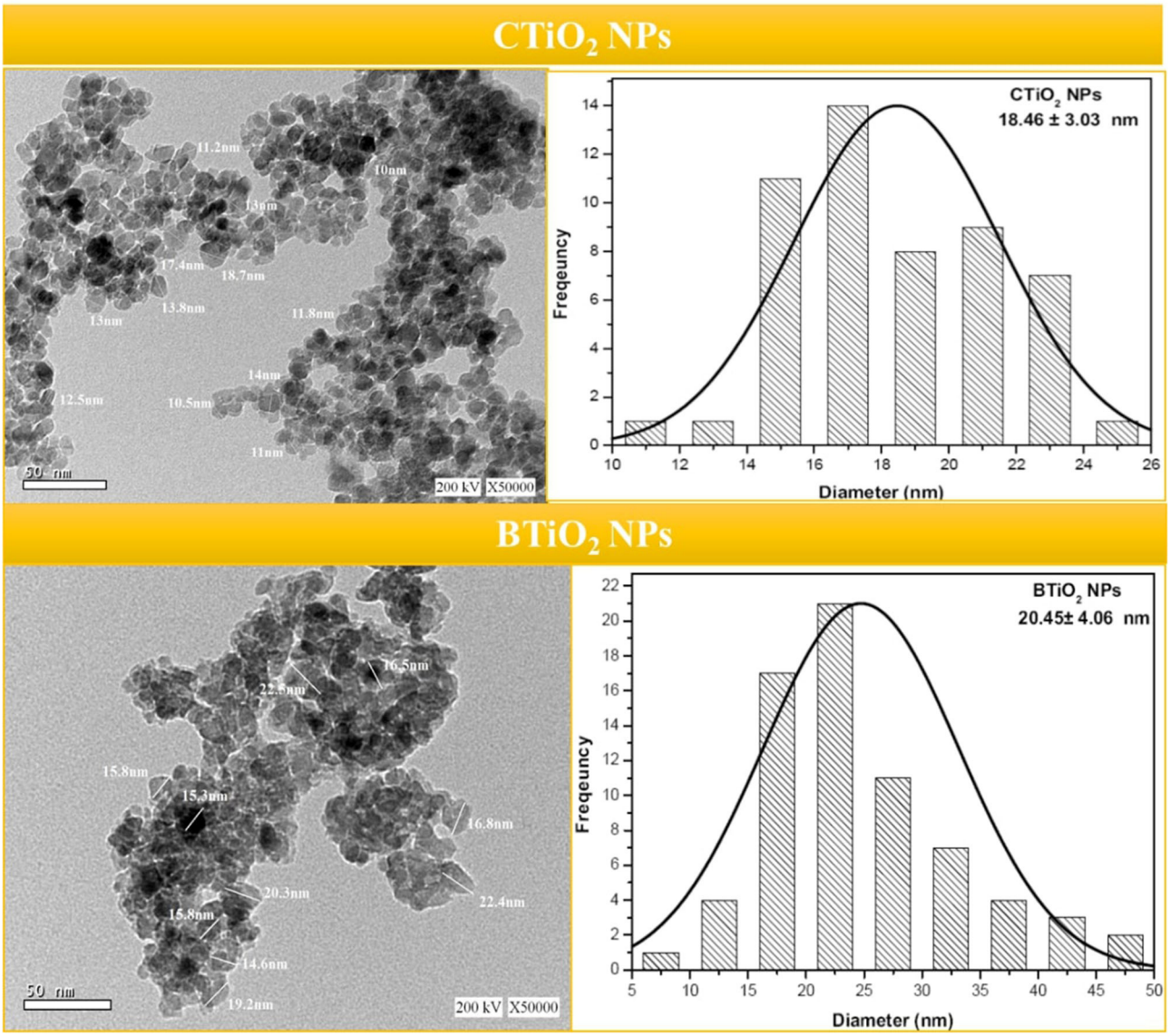

FIGURE 6
HRTEM images and particle size distribution of $BTiO_2$ and $CTiO_2$ NPs.

(48). Band 1631 cm^{-1} represents the Amid I: C=O stretching for proteins. Band 1412.5cm^{-1} represents the CH_2 vibration for lipids. The band at 1378.8 cm^{-1} represents the C=S stretching for sulfur compounds. The band at 1274.4 cm^{-1} represents the C-N stretching for amino acids. The band at 1120.5 cm^{-1} represents the C-N stretching for amino acids, symmetric C-H stretching, and the vibration presence of antioxidant enzymes. The band at 1025.6 cm^{-1} represents SO_3 symmetric stretching, mainly sulfur compounds. Bands at 931.2 cm^{-1} and 817.5 cm^{-1} represent the N-H stretching of proteins (49).

FTIR spectroscopy indicated the successful formation of TiO_2 NPs and the generation of the functional groups in garlic extract that are responsible for the reduction of Ti precursors. The FTIR spectrum of TiO_2 NPs is characterized by three broad bands, the first of which, between ~3800 and 3000 cm^{-1}, belongs to the stretching vibration of the hydroxyl group (O-H). The second band is around 1626 and 1638 cm^{1}, which belongs to the stretching of titanium. The third band, located approximately between 800 and 450 cm^{-1}, was the fingerprint of Ti-O stretching vibration. These bands were observed in all samples, which confirms the formation of TiO_2 NPs (50).

The biosynthesis of TiO_2 NPs using garlic extract was confirmed by the occurrence of functional groups in both TiO_2 and garlic. The functional groups of garlic at 1631 cm^{-1}, 1378.8 cm^{-1}, and 1120.5 cm^{-1} were shifted to the lower wave numbers such as 1623.6 cm^{-1}, 1377 cm^{-1}, and 1117.4 cm^{-1}, respectively. This reflects the presence of C=O, C=S, and C-N and symmetric C-H stretching vibrations of antioxidant enzymes in the formation of TiO_2-garlic NPs. The band at 417.7 cm^{-1} corresponds to the Ti–O –Ti. A vibrational band appeared around 716.8 cm^{-1} due to TiO_2 modes in the anatase phase (51). The bands assigned for C-H stretching, CH_2 vibration, and

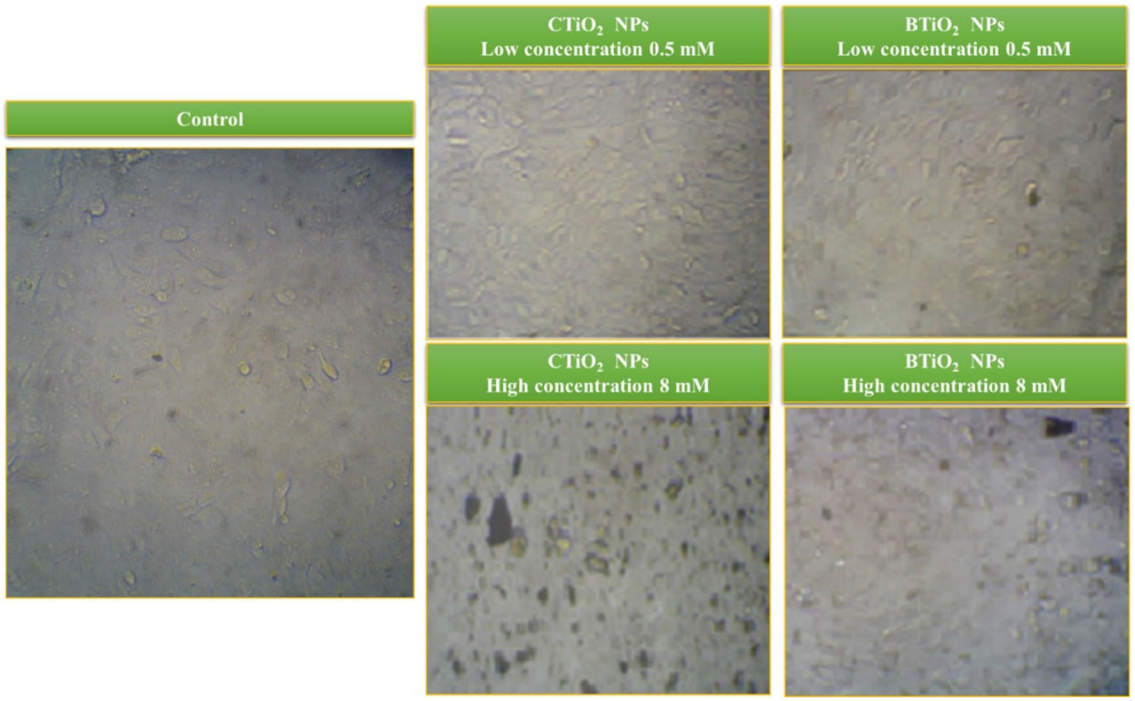

FIGURE 7
Microscopic images of $HepG_2$ cells after 24 h of exposure to $BTiO_2$ and $CTiO_2$ NPs at two concentrations (0.5 and 8 mM).

symmetric C-H stretching disappeared in biosynthesized TiO_2NPs. In addition, bands corresponding to C=O, C=S, and C-N appeared in biosynthetic TiO_2 NPs. Consequently, C=O, C=S, and C-N functional groups are the cause of the bioreduction of titanium isopropoxide to TiO_2NPs.

High-resolution transmission electron microscope

HRTEM images of $CTiO_2$ and $BTiO_2$ NPs reflect a sort of agglomeration with a spherical or irregular spherical shape (see Figure 5). Particle size distribution of $CTiO_2$ and $BTiO_2$ NPs (see Figure 5) is estimated from HRTEM images. HRTEM images of the prepared samples showed a sort of agglomeration with an increase in the particle size of $BTiO_2$ NPs compared to $CTiO_2$ NPs, which was attributed to the presence of the biomolecules as they attracted other molecules due to the electrostatic force on their surfaces. Similar results were also obtained in the previous report (52, 53).

The average size is 18.46 ± 3.03 and 35.64 ± 4.9 nm for $CTiO_2$ and $BTiO_2$ NPs, respectively. These values are smaller than the calculated values from XRD results (48.19 and 53.317) for $CTiO_2$ and $BTiO_2$ NPs, respectively. This variation in size may be due to the agglomeration of TiO_2 NPs (51). The crystallite size calculated from Scherer's equation is the apparent size, which does not equal to the particle size, especially in the case of polydisperse NPs with aggregation, such as TiO_2 NPs.

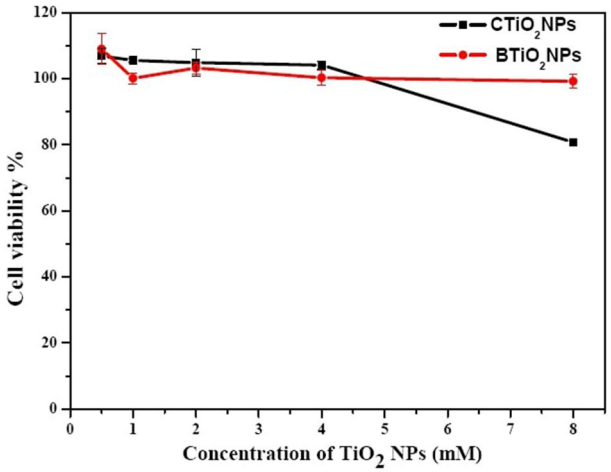

FIGURE 8
Cell viability of $HepG_2$ cells after 24 h of exposure to $BTiO_2$ and $CTiO_2$ NPs at two concentrations (0.5 and 8 mM).

Cytotoxicity

An accumulation of both TiO_2 NPs on the surface of the $HepG_2$ cells was found in the microscopic images (see Figure 6). Particularly, in the case of $CTiO_2$ NPs, this accumulation increased as NP concentration increased. The normalized cell viability is presented in Figure 7, and there is no observed toxicity for $CTiO_2$ and $BTiO_2$ NPs at low concentrations, while a small percentage of

toxicity was observed for $CTiO_2$ at high concentrations (8 mM), as shown in Figure 8.

The cytotoxicity of biosynthesized NPs can be tuned by several parameters, such as particle size, shape, and surface chemistry (54). It is reported that the biosynthesis of NPs can modify their surface due to the interaction with biomolecules, which, in turn, enhances the biocompatibility of the formed NPs (55). Similar behavior was observed in the cytotoxicity of our samples, as $BTiO_2$ NPs showed less toxic potential than $CTiO_2$ NPs. The accumulation of TiO_2 NPs on the surface of $HepG_2$ cells reduces the internalization rate and the cytotoxic effects (56–58).

Sequence variation using *16s rRNA* gene

Herein, we assess the potential genetic effects of oral exposure to chemically and biosynthesized TiO_2 NPs with two doses (100 and 300 mg/kg body weight/day) during pregnancy.

In mothers, 538–543 bp of nucleotide sequences were obtained. The obtained sequences were deposited into GenBank, and the accession numbers are MZ782915, MZ782917, MZ782918, MZ782919, and MZ782920. The percentages of nitrogen bases are shown in Table 1. In the embryo, 540–550 bp of nucleotide sequences were obtained. The obtained sequences of embryos were submitted to GenBank, and the accession numbers are MZ788644, MZ788646, MZ788647, MZ788648, and MZ788649. The percentages of nitrogen bases are shown in Table 2.

In mothers, the P-distance among the groups was 0.0000 to 0.0027%. The highest P-distance (0.0027) was found between the control group and C100–TiO_2 NPs groups (Table 3 and Figure 9). In the embryo, the P-distance among the groups was 0.00. Overall, the distance value among all groups was 0.000% (Table 4).

Histopathological examination of fetal kidney

Histological findings of kidney tissue stained by H&E exhibited intact renal architectures in the control embryos (Figure 10A). Contrariwise, C100–TiO_2 NPs mg/kg/day treated group showed necrosis of the renal tissues compensated by focal mononuclear infiltrate and separation of the epithelium-lining tubules (Figure 10B). Similarly, C300–TiO_2 NPs treated group displayed severe histological damage characterized by necrosed and desquamated epithelial cells with extensive inflammation (Figure 10C). Regarding B100–TiO_2 NPs, they showed apparently normal kidney parenchyma (Figure 10D). Moreover, treated group with B300–TiO_2 NPs revealed healthy renal tissues with mildly congested blood vessels (Figure 10E).

Discussion

Oral consumption of TiO_2 NPs is considered one of the most common exposure scenarios due to exposure to TiO_2 NPs found in

TABLE 1 Accession numbers, nucleotide frequencies, and their averages for *16S rRNA* gene in the five mother groups.

Group	Accession number	Base pair Length	Nucleotide Number%				A + T Content (%)	C + G Content (%)
			A%	T%	C%	G%		
Control	MZ782915	538.0	33.3	27.3	19.7	19.7	60.6	39.4
C100 – TiO_2 NPs	MZ782917	539.0	33.4	27.2	19.9	19.5	60.6	39.4
C300 – TiO_2 NPs	MZ782918	543.0	33.1	27.7	19.5	19.7	60.8	39.2
B100 – TiO_2 NPs	MZ782919	542.0	33.2	27.3	19.6	19.9	60.5	39.5
B300 – TiO_2 NPs	MZ782920	542.0	33.2	27.3	19.6	19.9	60.5	39.5
Average%		540.8	33.2	27.5	19.6	19.7	60.7	39.3

TABLE 2 Accession numbers, nucleotide frequencies, and their averages for *16S rRNA* gene in the embryo in five groups.

Group	Accession number	Base pair Length	Nucleotide number%				A + T Content (%)	C + G Content (%)
			A%	T%	C%	G%		
Control	MZ788644	540.0	33.4	27.4	19.6	19.6	60.8	39.2
C100 – TiO_2 NPs	MZ788646	540.0	33.4	27.4	19.6	19.6	60.8	39.2
C300 – TiO_2 NPs	MZ788647	546.0	33.2	28	19.4	19.4	61.2	38.8
B100 – TiO_2 NPs	MZ788648	550.0	33	28.2	19.3	19.5	61.2	38.8
B300 – TiO_2 NPs	MZ788649	550.0	33.3	28	19.3	19.4	61.3	38.7
Average%		544.3	33.3	27.7	19.5	19.5	61	39

TABLE 3 Pairwise distances among mother-five groups using *16S rRNA* gene.

Control		0.0027	0.0018	0.0018	0.0018
C100 – TiO_2 NPs	0.0037		0.0020	0.0020	0.0020
C300 – TiO_2 NPs	0.0019	0.0019		0.0019	0.0019
B100 – TiO_2 NPs	0.0019	0.0019	0.0018		0.0000
B300 – TiO_2 NPs	0.0019	0.0019	0.0018	0.0000	

Control	-	-	T	A	T	T	G
C100 – TiO_2 NPs	-	-	.	.	.	C	A
C300 – TiO_2 NPs	T	G	.	.	.	.	A
B100 – TiO_2 NPs	-	G	.	.	.	.	A
B300 – TiO_2 NPs	-	G	.	.	.	.	A

FIGURE 9
Alignment of *16S rRNA* partial sequences in mother-five groups. Dots refer to identical nucleotides, and A, T, C, and G refer to different nucleotides.

TABLE 4 Pairwise distances among embryonic five groups using *16S rRNA* gene.

Control		0.000	0.000	0.000	0.000
C100 – TiO_2 NPs	0.000		0.000	0.000	0.000
C300 – TiO_2 NPs	0.000	0.000		0.000	0.000
B100 – TiO_2 NPs	0.000	0.000	0.000		0.000
B300 – TiO_2 NPs	0.000	0.000	0.000	0.000	

food, liquid products, and medicines (20, 46). Due to the smaller size and physiochemical properties of TiO_2 NPs, different cytotoxic and genotoxic behaviors were detected. Previous studies have demonstrated that NPs might pass biological barriers. Following intravenous injection at GD 16–17, TiO_2 NPs (35 nm) and silica (70 nm) NPs passed the mature blood placenta barrier (59).

Furthermore, another study observed that orally administrated ZrO_2 might pass the intestinal and maternal blood placenta barriers, and nanoparticles would accumulate in the fetal brain after three repeated oral doses to late-pregnancy mice (GD 16, 17, and 18) (60).

In most multicellular organisms, the mitochondrial DNA is maternally inherited, meaning it is inherited from the mother (61). *16S rRNA* gene was primarily used for the identification of an organism, and thereafter, *16S rRNA* sequencing was able to reclassify the organism into completely new species or even genera (62).

When compared with GC, the entire *16S rRNA* gene exhibits AT richness (63). This was in coordination with our results, where the region amplified by the *16S rRNA* gene was AT-rich.

Based on the results of *16S rRNA* sequences of mothers, TiO_2 NPs caused genetic variation, where the TiO_2 NPs-treated groups were genetically distant from the control group that attributed to the effect of TiO_2 NPs. Landsiedel et al. (64) describe various studies on the genotoxicity of nanomaterials that contain TiO_2 NPs. They claim that the development of micronuclei, a sign of chromosomal and DNA damage, is evidence of the genotoxicity of TiO_2 NPs.

DNA damage can result from NPs that enter the body through the skin, mouth, or respiratory system. The oxidative stress and inflammation response associated with exposure to TiO_2 NPs can interrupt DNA structure, indirectly causing genetic effects. Being small enough, it can directly interact with DNA, causing genetic changes or even damaging the genetic material. When the nuclear membrane vanishes during mitosis, the entry of TiO_2 NPs into the nucleus is possible. The penetration of TiO_2 NPs and silica NPs into the nucleus was confirmed by many researchers. They reported that these small particles interact with intracellular proteins, causing aggregation, which can inhibit the replication, transcription, and proliferation processes (65, 66).

Some NPs can enter cell nuclei and may directly interfere with the structure and function of genomic DNA (67). TiO_2 NPs have been studied for their potential to cause cancer using assays that monitor gene mutations, chromosomal damage, indicative of potential clastogenic activity of the particles, and DNA strand breaks (29, 68–73). In the same context, TiO_2 NPs cause clastogenicity, genetic variation, oxidative DNA damage, and inflammation *in vivo* in mice. These outcomes were seen after just 5 days of water-based therapy (74).

On the contrary, the results of *16S rRNA* sequences in embryos did not display differences between the control group and the TiO_2 NP-treated ones, which reflected that the TiO_2 NPs did not affect the genetic structure of the embryos. This is in coordination with the previous report (30) which reported that at doses up to 1000 mg/kg/day, there was no evidence of toxicity in the maternal or developmental tissues.

On the other hand, the histopathological findings showed that the embryonic renal tissue of the CTiO_2 NP-treated group showed significant necrosis compensated by focal mononuclear infiltrate, in addition to the separation of epithelium-lining tubules (75). The results indicate that exposure to BTiO_2 NPs reduced damage in the kidney tissue of the embryo. These results provide evidence that the biosynthesis of NPs can modify their surface due to the interaction with biomolecules, which, in turn, enhances the biocompatibility of the formed NPs.

The results of this study will provide worthy information on the developmental genotoxicity of CTiO_2 NPs and BTiO_2 NPs *via* repeated oral exposure, which can help in the process of hazard estimation of widely used nanoparticles.

Conclusion

Titanium dioxide NPs were biosynthesized with garlic extract as a reducing agent and have a semispherical shape. The biosynthesized protein did not show any structural disorder except for the increase in particle size, which, in turn, caused a

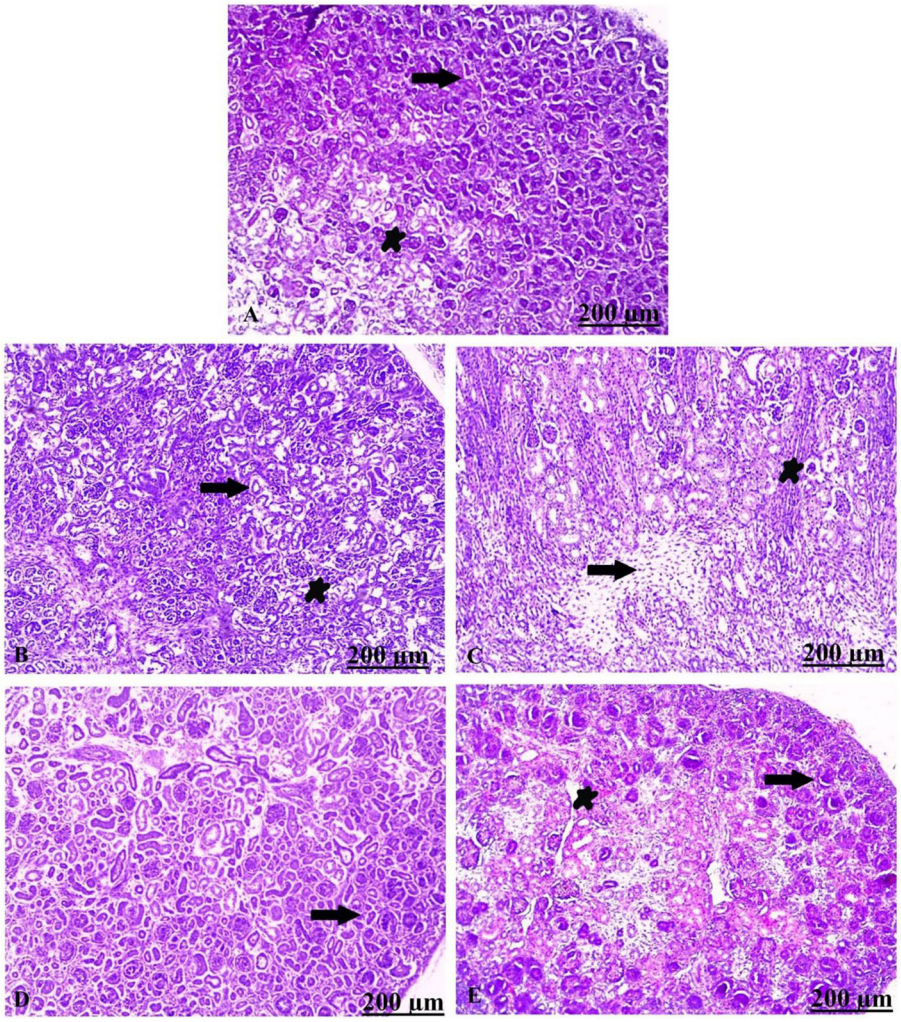

FIGURE 10
(A–E) Transverse sections stained with H&E from fetal kidney of control (untreated) and experimental (treated) groups: **(A)** Light section of control showing intact nephritic tubules (arrow) and glomerulus (star). **(B)** Light section of C100–TiO_2 NPs showing separation of epithelium-lining tubules from the basement membrane (arrow), besides mononuclear infiltrate (star). **(C)** Light section of C300–TiO_2 NPs showing necrosis of the renal tubules replaced by inflammatory cells (arrow) as well as desquamated epithelial cells (star). **(D)** Light section of B100–TiO_2 NPs showing apparently healthy renal parenchyma (arrow). **(E)** Light section of B300–TiO_2 NPs showing healthy glomeruli (arrow) and mild congestion of the renal blood vessels (star). Scale bar = 200 µm.

little decrease in its cytotoxicity against $HepG_2$ cells. Moreover, the results of *16S rRNA* sequences of mother groups showed that chemically synthesized TiO_2 NPs caused genetic variation compared to the control. The results of the maternal study showed that the biosynthesized TiO_2 NPs were less toxic compared to chemically synthesized TiO_2 NPs. However, the embryo-treated groups with both chemically and biosynthesized TiO_2 NPs did not display any differences compared to the control group. Our study was mainly designed for the experimental use of TiO_2 NPs and not for food or cosmetics; we recommend that the genetic variation be investigated more carefully.

Data availability statement

The original contributions presented in the study are included in the article/supplementary material, further inquiries can be directed to the corresponding authors.

Ethics statement

The animal study was reviewed and approved by the Ethics of Animal Experiments Committee of South Valley University, Faculty of Science (Permit Number: 002/9/22).

Author contributions

ZK and AS: conception of the idea of the manuscript. ZK, AS, AE, IR, FZ, ZF, and MA: conceptualization and methodology. ZK, AS, AE, IR, FZ, ZF, and MA: formal analysis, writing, reviewing, and editing. All authors have substantially contributed to each step of manuscript preparation, study procedure, contributed to the article, and approved the submitted version.

Funding

This study was supported by the Slovak project KEGA no. 009UVLF-4/2021: Innovation and implementation of new knowledge of scientific research and breeding practice to improve the teaching of foreign students on the subject of animal husbandry.

Conflict of interest

The authors declare that the research was conducted in the absence of any commercial or financial relationships that could be construed as a potential conflict of interest.

Publisher's note

All claims expressed in this article are solely those of the authors and do not necessarily represent those of their affiliated organizations, or those of the publisher, the editors and the reviewers. Any product that may be evaluated in this article, or claim that may be made by its manufacturer, is not guaranteed or endorsed by the publisher.

References

1. Sargent J. Nanotechnology: a policy primer. *CRS Report*. (2012). Available at: https://www.everycrsreport.com/files/20120413_RL34511_ff61c3e95212b3df695ffa0a43feae4cd3081e23.pdf (accessed September 15, 2016).

2. Borm PJA. and Berube D. A tale of opportunities, uncertainties, and risks. *Nanotoday*. (2008) 3:56–9. doi: 10.1016/S1748-0132(08)70016-1

3. Hendren CO, Mesnard X, Dröge J, Wiesner MR. Estimating production data for five engineered nanomaterials as a basis for exposure assessment. *Environ Sci Technol*. (2011) 45:4190. doi: 10.1021/es2009924

4. Sharifi S, Behzadi S, Laurent S, Laird Forrest M, Stroeve P, Mahmoudi M. Toxicity of nanomaterials. *Chem Soc Rev*. (2012) 41:2323–43. doi: 10.1039/C1CS15188F

5. Sadhasivam S, Shanmugam M, Umamaheswaran PD, Venkattappan A, Shanmugam A. Zinc oxide nanoparticles: green synthesis and biomedical applications. *J Clust Sci*. (2021) 32:1441–55. doi: 10.1007/s10876-020-01918-0

6. Chan S. Biosynthesis of metal oxide nanoparticles. *ChemBioEng Rev*. (2016) 3:55–67. doi: 10.1002/cben.201500018

7. Gour A, Jain NK. Advances in green synthesis of nanoparticles. *Artif Cells, Nanomed Biotechnol*. (2019) 47:844–51. doi: 10.1080/21691401.2019.1577878

8. Thamima M, Karuppuchamy S. Biosynthesis of titanium dioxide and zinc oxide nanoparticles from natural sources: a review. *Adv Sci Eng Med*. (2015) 7:18–25. doi: 10.1166/asem.2015.1648

9. Bekele ET, Gonfa BA, Sabir FK. Use of different natural products to control growth of titanium oxide nanoparticles in green solvent emulsion, characterization, and their photocatalytic application. *Bioinorg Chem Appl*. (2021) 2021:6626313. doi: 10.1155/2021/6626313

10. Sorbiun M, Shayegan Mehr E, Ramazani A, Mashhadi Malekzadeh A. Biosynthesis of metallic nanoparticles using plant extracts and evaluation of their antibacterial properties. *Nanochemistry Res*. (2018) 3:1–16.

11. Li S, Shen Y, Xie A, Yu X, Qiu L, Zhang L, et al. Green synthesis of silver nanoparticles using *Capsicum annuum* L. *extract Green Chem*. (2007) 9:852–8. doi: 10.1039/b615357g

12. Iravani S. Green synthesis of metal nanoparticles using plants. *Green Chem*. (2011) 13:2638–50. doi: 10.1039/c1gc15386b

13. Makarov VV, Love AJ, Sinitsyna OV, Makarova SS, Yaminsky IV, Taliansky ME, et al. "Green" nanotechnologies: synthesis of metal nanoparticles using plants. *Acta Naturae*. (2014) 6:35–44. doi: 10.32607/20758251-2014-6-1-35-44

14. Huang J, Lin L, Sun D, Chen H, Yang D, Li Q. Bio-inspired synthesis of metal nanomaterials and applications. *Chem Soc Rev*. (2015) 44:6330–74. doi: 10.1039/C5CS00133A

15. Hirakawa K, Mori M, Yoshida M, Oikawa S, Kawanishi S. Photo-irradiated titanium dioxide catalyzes site specific DNA damage via generation of hydrogen peroxide. *Free Radic Res*. (2004) 38:439–47. doi: 10.1080/10715762042000206487

16. Gonçalves DM, Chiasson S, Girard D. Activation of human neutrophils by titanium dioxide (TiO2) nanoparticles. *Toxicol In Vitro*. (2010) 24:1002–8. doi: 10.1016/j.tiv.2009.12.007

17. Reeves JF, Davies SJ, Dodd NJF, Jha AN. Hydroxyl radicals (*OH) are associated with titanium dioxide [TiO_2)] nanoparticle-induced cytotoxicity and oxidative DNA damage in fish cells. *Mutat Res*. (2008) 640:113–22. doi: 10.1016/j.mrfmmm.2007.12.010

18. Kang SJ, Kim BM, Lee YJ, Hong SH, Chung HW. Titanium dioxide nanoparticles induce apoptosis through the JNK/p38-caspase-8-Bid pathway in phytohemagglutinin-stimulated human lymphocytes. *Biochem Biophys Res Commun*. (2009) 386:682–7. doi: 10.1016/j.bbrc.2009.06.097

19. Yu Y, Ren W, Ren B. Nanosize titanium dioxide cause neuronal apoptosis: a potential linkage between nanoparticle exposure and neural disorder. *Neurol Res*. (2008) 30:1115–20. doi: 10.1179/0161641215Z.000000000587

20. Kamal Z, Ebnalwaled AA, Al-amgad Z, Ondrašovi? S, Rehan IF. Ameliorative e ect of biosynthesized titanium dioxide nanoparticles using garlic extract on the body weight and developmental toxicity of liver in albino rats compared with chemically synthesized nanoparticles. *Front Vet*. (2022) 9:1049817. doi: 10.3389/fvets.2022.1049817

21. Kamal Z, Zeinab AAE, Amgad A, Saied AA, Metwally AA. Immunomodulatory and antioxidant effect of green synthesized titanium dioxide nanoparticles on pregnant female albino rats and their fetuses. *Environ Sci Pollut Res*. (2023) 30:5554–75. doi: 10.1007/s11356-023-26264-2

22. Scown TM, van Aerle R, Johnston BD, Cumberland S, Lead JR, Owen R, et al. High doses of intravenously administered titanium dioxide nanoparticles accumulate in the kidneys of rainbow trout but with no observable impairment of renal function. *Toxicol Sci*. (2009) 109:372–80. doi: 10.1093/toxsci/kfp064

23. Qin L, Wine-Lee L, Ahn KJ, Crenshaw EB. Genetic analyses demonstrate that bone morphogenetic protein signaling is required for embryonic cerebellar development. *J Neurosci*. (2006) 26:1896–905. doi: 10.1523/JNEUROSCI.3202-05.2006

24. Jin C-Y, Zhu B-S, Wang X-F, Lu Q-H. Cytotoxicity of titanium dioxide nanoparticles in mouse fibroblast cells. *Chem Res Toxicol*. (2008) 21:1871–7. doi: 10.1021/tx800179f

25. Bu Q, Yan G, Deng P, Peng F, Lin H, Xu Y et al. NMR-based metabonomic study of the sub-acute toxicity of titanium dioxide nanoparticles in rats after oral administration. *Nanotechnology*. (2010) 21:125105. doi: 10.1088/0957-4484/21/12/125105

26. Shakeel M, Jabeen F, Shabbir S, Asghar MS, Khan MS CA. Toxicity of nano-titanium dioxide (TiO2-NP) through various routes of exposure: a review. *Biol Trace Elem Res*. (2016) 172:1–36. doi: 10.1007/s12011-015-0550-x

27. Shubha P, Namratha K, Gowda ML, Nayan M, Manjunatha H, Byrappa K. In vitro and in vivo toxicological evaluation of green synthesised anatase TiO_2 nanoforms. *Mat Res Innov*. (2023) 7:138–44. doi: 10.1080/14328917.2022.2094629

28. Irshad MA, Nawaz R, Rehman MZ ur, Adrees M, Rizwan M, Ali S. Synthesis, characterization and advanced sustais of titanium dioxide nanoparticles: A review. *Ecotoxicol Environ Saf*. (2021) 25:212. doi: 10.1016/j.ecoenv.2021.111978

29. Wang JJ, Sanderson BJS, Wang H. Cyto- and genotoxicity of ultrafine TiO_2 particles in cultured human lymphoblastoid cells. *Mutat Res*. (2007) 628:99–106. doi: 10.1016/j.mrgentox.2006.12.003

30. Warheit DB, Boatman R, Brown SC. Developmental toxicity studies with 6 forms of titanium dioxide test materials (3 pigment-different grade & 3 nanoscale) demonstrate an absence of effects in orally-exposed rats. *Regul Toxicol Pharmacol*. (2015) 73:887–96. doi: 10.1016/j.yrtph.2015.09.032

31. Lee J, Jeong J-S, Kim SY, Park M-K, Choi S-D, Kim U-J, et al. Titanium dioxide nanoparticles oral exposure to pregnant rats and its distribution. *Part Fibre Toxicol*. (2019) 16:1–12. doi: 10.1186/s12989-019-0313-5

32. World Health Organization (WHO). *FAO Nutrition Meetings Report Series No. 46A: 1969. Toxicological Evaluation of Some Food Colours, Emulsifiers, Stabilizers, Anti-Caking Agents and Certain Other Substances*. Geneva: WHO/ FOOD ADD/70.36 (1969).

33. Hu R, Gong X, Duan Y, Li N, Che Y, Cui Y, et al. Neurotoxicological effects and the impairment of spatial recognition memory in mice caused by exposure to TiO2 nanoparticles. *Biomaterials*. (2010) 31:8043–50. doi: 10.1016/j.biomaterials.2010.07.011

34. Simon C, Franke A. Martin AP. The polymerase chain reaction: DNA extraction and amplification. *Mol Tech Taxon.* (1991) 57:329–55. doi: 10.1007/978-3-642-83962-7_22

35. Thompson JD, Higgins DG, Gibson TJ. Clustal W. Improving the sensitivity of progressive multiple sequence alignment through sequence weighting, position-specific gap penalties and weight matrix choice. *Nucleic Acids Res.* (1994) 22:4673–80. doi: 10.1093/nar/22.22.4673

36. William JB, Linda MB. Color Atlas of Veterinary Histology. Hoboken, NJ: Blackwell Publishing (2000)

37. Zhang Q, Wu Y, Zuo T. Green recovery of titanium and effective regeneration of TiO_2 photocatalysts from spent selective catalytic reduction catalysts. *ACS Sustain Chem Eng.* (2018) 6:3091–101. doi: 10.1021/acssuschemeng.7b03038

38. Ahmad MA, Yuesuo Y, Ao Q, Adeel M, Hui ZY, Javed R. Appraisal of comparative therapeutic potential of undoped and nitrogen-doped titanium dioxide nanoparticles. *Molecules.* (2019) 24:1–15. doi: 10.3390/molecules24213916

39. Ahamed M, Khan MAM, Akhtar MJ, Alhadlaq HA, Alshamsan A. Ag-doping regulates the cytotoxicity of TiO_2 nanoparticles via oxidative stress in human cancer cells. *Sci Rep.* (2017) 7:1–14. doi: 10.1038/s41598-017-17559-9

40. Bassi AL, Cattaneo D, Russo V, Bottani CE, Barborini E, Mazza T, et al. Raman spectroscopy characterization of titania nanoparticles produced by flame pyrolysis: The influence of size and stoichiometry. *J Appl Phys.* (2005) 98:074305. doi: 10.1063/1.2061894

41. Zhang WF, He1 YL, Zhang MS, Yin Z, Chen Q. Raman scattering study on anatase TiO_2 nanocrystals. *J Phys D Appl Phys.* (2000) 33:912–6. doi: 10.1088/0022-3727/33/8/305

42. Rahim S, Sasani Ghamsari M, Radiman S. Surface modification of titanium oxide nanocrystals with PEG. *Sci Iran.* (2012) 19:948–53. doi: 10.1016/j.scient.2012.03.009

43. Sabzi M, Mirabedini SM, Zohuriaan-Mehr J, Atai M. Surface modification of TiO_2 nano-particles with silane coupling agent and investigation of its effect on the properties of polyurethane composite coating. *Prog Org Coatings.* (2009) 65:222–8. doi: 10.1016/j.porgcoat.2008.11.006

44. Zhao J, Milanova M, Warmoeskerken MMCG, Dutschk V. Surface modification of TiO_2 nanoparticles with silane coupling agents. *Colloids Surf Physicochem Eng Asp.* (2012) 413:273–9. doi: 10.1016/j.colsurfa.2011.11.033

45. Abazović ND, Comor MI, Dramićanin MD, Jovanović DJ, Ahrenkiel SP, Nedeljković JM. Photoluminescence of anatase and rutile TiO_2 particles. *J Phys Chem B.* (2006) 110:25366–70. doi: 10.1021/jp064454f

46. Mugundan S, Rajamannan B, Viruthagiri G, Shanmugam N, Gobi R, Praveen P. Synthesis and characterization of undoped and cobalt-doped TiO_2 nanoparticles via sol–gel technique. *Appl Nanosci.* (2015) 5:449–56. doi: 10.1007/s13204-014-0337-y

47. Devanand Venkatasubbu G, Ramasamy S, Ramakrishnan V, Kumar J. Folate targeted PEGylated titanium dioxide nanoparticles as a nanocarrier for targeted paclitaxel drug delivery. *Adv Powder Technol.* (2013) 24:947–54. doi: 10.1016/j.apt.2013.01.008

48. Divya BJ, Suman B, Venkataswamy M, Thyagaraju K. A Study On phytochemicals, functional groups and mineral composition of *Allium sativum* (garlic) cloves. *Int J Curr Pharm Res.* (2017) 9:888. doi: 10.22159/ijcpr.2017.v9i3.18888

49. Nagarajan D, Kumar TR. Fourier transform infrared spectroscopy analysis of garlic (Allium). *Int J Zoo Stud.* (2017) 2:11–4.

50. Al-Shabib NA, Husain FM, Qais FA, Ahmad N, Khan A, Alyousef AA. Phyto-mediated synthesis of porous titanium dioxide nanoparticles from withania somnifera root extract: Broad-spectrum attenuation of biofilm and cytotoxic properties against $HepG_2$ cell lines. *Front Microbiol.* (2020) 11:1680. doi: 10.3389/fmicb.2020.01680

51. Órdenes-Aenishanslins NA, Saona LA, Durán-Toro VM, Monrás JP, Bravo DM, Pérez-Donoso JM. Use of titanium dioxide nanoparticles biosynthesized by Bacillus mycoides in quantum dot sensitized solar cells. *Microb Cell Fact.* (2014) 13:1–10. doi: 10.1186/s12934-014-0090-7

52. Arabi N, Kianvash A, Hajalilou A, Abouzari-Lotf E, Abbasi-Chianeh V, A. facile and green synthetic approach toward fabrication of Alcea- and Thyme-stabilized TiO_2 nanoparticles for photocatalytic applications. *Arab J Chem.* (2020) 13:2132–41. doi: 10.1016/j.arabjc.2018.03.014

53. Shanavas S, Priyadharsan A, Karthikeyan S, Dharmaboopathi K, Ragavan I, Vidya C, et al. Green synthesis of titanium dioxide nanoparticles using Phyllanthus niruri leaf extract and study on its structural, optical and morphological properties. *Mater Today Proc.* (2020) 26:3531–4. doi: 10.1016/j.matpr.2019.06.715

54. Rejman J, Nazarenus M, Aberasturi DJ de, Said AH, Feliu N, Parak WJ. Some thoughts about the intracellular location of nanoparticles and the resulting consequences. *J Colloid Interface Sci.* (2016) 482:260–6. doi: 10.1016/j.jcis.2016.07.065

55. Hashem M, Al-Karagoly H. Synthesis, Characterization, and Cytotoxicity of Titanium dioxide nanoparticles and in vitro study of its impact on lead concentrations in bovine blood and milk. *J Biotech Res.* (2021) 12:93–105.

56. Khan AO, Di Maio A, Guggenheim EJ, Chetwynd AJ, Pencross D, Tang S. Surface chemistry-dependent evolution of the nanomaterial corona on TiO_2 nanomaterials following uptake and sub-cellular localization. *Nanomaterials.* (2020) 10:401. doi: 10.3390/nano10030401

57. Dalai S, Pakrashi S, Kumar RSS, Chandrasekaran N, Mukherjee A, A. comparative cytotoxicity study of TiO_2 nanoparticles under light and dark conditions at low exposure concentrations. *Toxicol Res.* (2012) 1:116–30. doi: 10.1039/c2tx00012a

58. Valentini X, Deneufbourg P, Paci P, Rugira P, Laurent S, Frau A, et al. Morphological alterations induced by the exposure to TiO_2 nanoparticles in primary cortical neuron cultures and in the brain of rats. *Toxicol Reports.* (2018) 5:878–89. doi: 10.1016/j.toxrep.2018.08.006

59. Yamashita K, Yoshioka Y, Higashisaka K, Mimura K, Morishita Y, Nozaki M, et al. Silica and titanium dioxide nanoparticles cause pregnancy complications in mice. *Nat Nanotechnol.* (2011) 6:321–8. doi: 10.1038/nnano.2011.41

60. Wang Z, Zhang C, Liu X, Huang F, Wang Z, Yan B. Oral intake of ZrO_2 nanoparticles by pregnant mice results in nanoparticles' deposition in fetal brains. *Ecotoxicol Environ Saf.* (2020) 202:884. doi: 10.1016/j.ecoenv.2020.110884

61. Szalai C, László V, Pap E, Tóth S, Falus A, Oberfrank F. *Medical Genetics and Genomics.* Budapest University of Technology and Economics (2016).

62. Weisburg WG, Barns SM, Pelletier DA, Lane DJ. 16S ribosomal DNA amplification for phylogenetic study. *J Bacteriol.* (1991) 173:697–703. doi: 10.1128/jb.173.2.697-703.1991

63. Bo Z, Xu T, Wang R, Jin X, Sun Y. Complete mitochondrial genome of the Bombay duck Harpodon nehereus (Aulopiformes, Synodontidae). *Mitochondrial DNA.* (2013) 24:660–2. doi: 10.3109/19401736.2013.772988

64. Landsiedel R, Kapp M, Schulz M, Wiench K, Oesch F. Genotoxicity investigations on nanomaterials: Methods, preparation and characterization of test material, potential artifacts and limitations—Many questions, some answers. *Mutat Res.* (2009) 681:241–58. doi: 10.1016/j.mrrev.2008.10.002

65. Fröhlich E. The role of surface charge in cellular uptake and cytotoxicity of medical nanoparticles. *Int J Nanomedicine.* (2012) 7:5577–91. doi: 10.2147/IJN.S36111

66. Magdolenova Z, Bilaničová D, Pojana G, Fjellsbø LM, Hudecova A, Hasplova K, et al. Impact of agglomeration and different dispersions of titanium dioxide nanoparticles on the human related in vitro cytotoxicity and genotoxicity. *J Environ Monit.* (2012) 14:455–64. doi: 10.1039/c2em10746e

67. Chen M, von Mikecz A. Formation of nucleoplasmic protein aggregates impairs nuclear function in response to SiO_2 nanoparticles. *Exp Cell Res.* (2005) 305:51–62. doi: 10.1016/j.yexcr.2004.12.021

68. Driscoll KE, Deyo LC, Carter JM, Howard BW, Hassenbein DG, Bertram TA. Effects of particle exposure and particle-elicited inflammatory cells on mutation in rat alveolar epithelial cells. *Carcinogenesis.* (1997) 18:423–30. doi: 10.1093/carcin/18.2.423

69. Warheit DB, Hoke RA, Finlay C, Donner EM, Reed KL, Sayes CM. Development of a base set of toxicity tests using ultrafine TiO2 particles as a component of nanoparticle risk management. *Toxicol Lett.* (2007) 171:99–110. doi: 10.1016/j.toxlet.2007.04.008

70. Gurr J-R, Wang ASS, Chen C-H, Jan K-Y. Ultrafine titanium dioxide particles in the absence of photoactivation can induce oxidative damage to human bronchial epithelial cells. *Toxicology.* (2005) 213:66–73. doi: 10.1016/j.tox.2005.05.007

71. Kang SJ, Kim BM, Lee YJ, Chung HW. Titanium dioxide nanoparticles trigger p53-mediated damage response in peripheral blood lymphocytes. *Environ Mol Mutagen.* (2008) 49:399–405. doi: 10.1002/em.20399

72. Linnainmaa K, Kivipensas P, Vainio H. Toxicity and cytogenetic studies of ultrafine titanium dioxide in cultured rat liver epithelial cells. *Toxicol In Vitro.* (1997) 11:329–35. doi: 10.1016/S0887-2333(97)00000-3

73. Rahman Q, Lohani M, Dopp E, Pemsel H, Jonas L, Weiss DG, et al. Evidence that ultrafine titanium dioxide induces micronuclei and apoptosis in Syrian hamster embryo fibroblasts. *Environ Health Perspect.* (2002) 110:797–800. doi: 10.1289/ehp.02110797

74. Trouiller B, Reliene R, Westbrook A, Solaimani P, Schiestl RH. Titanium dioxide nanoparticles induce DNA damage and genetic instability in vivo in mice. *Cancer Res.* (2009) 69:8784–9. doi: 10.1158/0008-5472.CAN-09-2496

75. Gui S, Zhang Z, Zheng L, Cui Y, Liu X. Molecular mechanism of kidney injury of mice caused by exposure to titanium dioxide nanoparticles. *J Hazard Mater.* (2011) 195:365–70. doi: 10.1016/j.jhazmat.2011.08.055